Nanoregions of Rock Salt AgI in AgBr Matrix

Jeffrey C. Hansen, Alfred P. Marchetti, Samuel Chen, Mark Irving, Roger Baetzold, and Byron R. Sever
Eastman Kodak Company
Rochester, New York/USA

Abstract

Rapid addition of iodide causes the optically excited, low-temperature donor-acceptor luminescence from $AgBr_{1-x}I_x$ (x < 0.4) microcrystals to shift to ≈580 nm, whereas this luminescence is observed between 530 to 540 nm in microcrystals with homogeneous iodide incorporation. The band-gap energy in rapid iodide addition microcrystals is ≈0.1 eV smaller than the measured band-gap energy for iodide concentrations near the maximum solubility (≈40%), even when the total iodide content is only a few percent. Low-temperature photoluminescence and excitation spectroscopy, transmission electron microscopy (TEM), and computational methods have been applied to determine the structure responsible for this behavior. The data generated indicates that nanoregions of fcc "rock salt" $AgBr_{1-x}I_x$ (x > 0.9) are integrated into these microcrystals. These nanoregions of high iodide are strained and can engender the characteristic dislocations observed in the TEMs. Some dislocation features are removed by annealing (200 ºC). Heating also causes the luminescence and band-gap energy to return to the values characteristic of the crystals with a homogeneous distribution of iodide.

Introduction

AgBr/I microcrystals are widely used in photographic products. At present, most color negative films contain AgBr microcrystals with some sort of iodide phase, either from a homogeneous (slow) addition of iodide or from a rapid iodide addition (RIA) step in their fabrication.[1] The homogeneous AgBr/I system forms an amalgamation semiconductor up to the solubility limit at about 40% iodide.[2,3] The low-temperature optical absorption and luminescence spectra, and the ESCA data indicate that the valence band is shifted up in energy as the iodide level is increased.[3-5] The low-temperature photoluminescence (LTPL) from samples with a homogeneous iodide distribution was found to peak between 525 and 540 nm, depending on the iodide concentration. It has been shown that RIA microcrystals have a LTPL luminescence band at ≈580 nm that is characteristic of this manner of iodide addition.[6] The LTPL from RIA microcrystals appears to be due to some feature other than levels of iodide below the solubility limit.[3] In addition, experimental band-gap energies from melt-grown samples up to $AgBr_{0.75}I_{0.25}$ were larger by ≈ 0.1 eV than those measured in RIA microcrystals.

It is the purpose of this article to present evidence that the species responsible for this LTPL characteristic observed in RIA microcrystals are metastable nanoregions of δ-AgI, which is the high pressure fcc (rock salt) phase. Data suggests that these regions trap holes and the inclusion of these nanoregions of δ−AgI contribute to the formation of some types of dislocations that are observed in transmission electron microscopy (TEM) of RIA microcrystals.

Experimental

The AgBr/I microcrystal dispersions were fabricated by a double jet addition of solutions of $AgNO_3$ and NaBr(KI) to a stirred reaction vessel containing gelatin. Additional details have been described previously.[7] Regions with homogeneous levels of iodide were created in microcrystals by precipitation with mixed bromide and iodide solutions. The concentrations of iodide ranged from 1% to greater than 25%. Iodide concentrations were calculated from the stoichiometry and confirmed by neutron activation analysis.

The RIA microcrystals were created by the addition of AgI nanocrystals or by a solution of KI, and the precipitation was completed using $AgNO_3$ and NaBr solutions.[8] Aliquots taken from the precipitation reactor just after the rapid KI addition confirmed the spectroscopic presence of AgI. When added rapidly, the amount of iodide constitutes only a few percent of the total halide. Band-gap energies were obtained from a large number of "melt-grown" and microcrystalline samples. Two examples are detailed here. 1.5 × 0.1 μm (diameter × thickness) $AgBr_{0.97}I_{0.03}$ tabular microcrystal dispersions were prepared for comparison. The first is a homogeneous iodide microcrystal dispersion having a local iodide concentration of 6 mol % for 50% of the fabrication. The second is an RIA microcrystal dispersion with a 3% AgI addition.

The LTPL measurement apparatus and experimental procedures have been described previously.[7,10] After gelatin removal, the microcrystals were placed in a furnace at temperature for one hour.

The data on the band-gap energies of the $AgBr_{1-x}I_x$ melt-grown crystals were taken from Ref. 3. The method of obtaining the band-gap energy from excitation spectra is straightforward and has been described elsewhere.[7]

Microcrystal dispersions with known homogeneous levels of iodide, along with several different melt-grown samples were used to check the excitation method for obtaining band-gap energies. The uncertainty in the direct absorption measurements was thought to be ±5 meV, while the measurements from the excitation spectra was ±10 meV. Room temperature band-gap energies were obtained on some microcrystal dispersions by measuring their diffuse reflectance spectra and transforming these data, with the Kubelka-Munk relation, to derive data proportional to the optical density. The band-gap energy for face-centered cubic (fcc) AgI has previously been determined as a function of pressure.[10] The room temperature value is 2.26 eV at the transition pressure of 7 kbar (0.7 GPa) with a lattice constant of 6.067 Å. The band-gap energy decreases with increasing pressure and has a pressure dependence of –61 meV/GPa.

Transmission and analytical electron microscopic analysis of $AgBr_{1-x}I_x$ tabular microcrystals, as well as the methods for preparing cryogenic cross-sections, have been described previously.[11]

Computation

Atomistic modeling techniques have been successfully used to study various bulk electronic and surface structural properties of AgCl and AgBr.[12,13] In this paper, the stability of small clusters of AgI within the bulk fcc AgBr crystal lattice is studied. However, potentials for wurtzite AgI did not exist prior to this work and are generated here.[7] To include possible covalent interactions in this material, it is necessary to include three-body bond harmonic terms to the potential for Ag-I-I, I-Ag-Ag, and Ag-Ag-Ag components. The parameters for the AgI potential were obtained by fitting to the structure and elastic constants and are tabulated in Ref7 the values for the AgBr potential are taken from Ref. 1 Application of Random-Dot Model-to-Fog Granularity Caused by High-Energy Radiation of Silver Halide Emulsions in Color Systems 4.

The general utilities lattice program (GULP) is used to calculate the stability of AgI units within the AgBr crystal.[15] This code is based upon the Mott-Littleton procedure and employs a region around the central AgI cluster in which all ions are fully treated and surrounded by a second spherical region in which ions are treated by the harmonic part of the potential. The rest of the crystal is treated by continuum methods. A complete description of the method may be found in Ref. 15.

Results and Discussions

Figure 1 compares the LTPL and excitation spectra obtained from dispersions of RIA and homogeneous iodide tabular microcrystals of composition $AgBr_{0.97}I_{0.03}$. The homogeneous iodide microcrystals exhibit a single luminescence band at ≈540 nm, which is due to donor acceptor (DA) recombination within the bromoiodide phase. For the RIA microcrystals, the dominant luminescence band is observed at ≈580 nm. This is the signature of an RIA procedure and has been associated with a unique bromoiodide phase. Microcrystals of cubic and octahedral morphology fabricated with an RIA step also have a LTPL peaking at ≈580 nm.

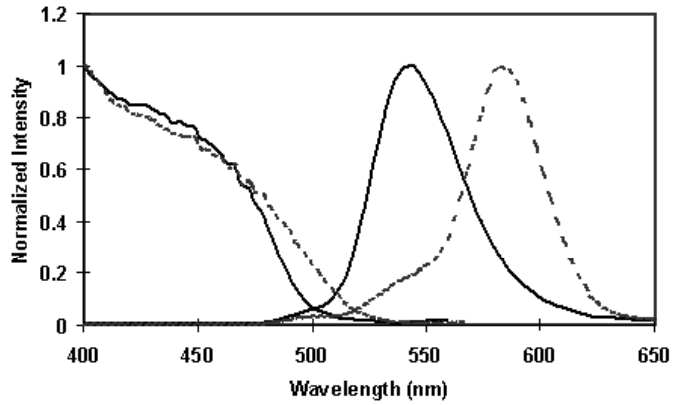

Figure 1. The luminescence and excitation spectra of tabular microcrystals having homogeneous iodide (solid) and RIA from AgI seed addition (dashed). Total bulk iodide content is 3%.

The effects of annealing on luminescence from the RIA sample are shown in Fig. 2. Even after the lowest temperature annealing at 120 °C, much of the RIA-related luminescence at 580 nm has shifted to 540 nm, indicating the unique defect character of the RIA region has been significantly modified. For the 120 and 160 °C treatments, the RIA luminescence remains observable at 580 nm, indicating that not all of the RIA "defect" character was changed. For the 200 °C treatment, only a slight extension on the long wavelength side of the

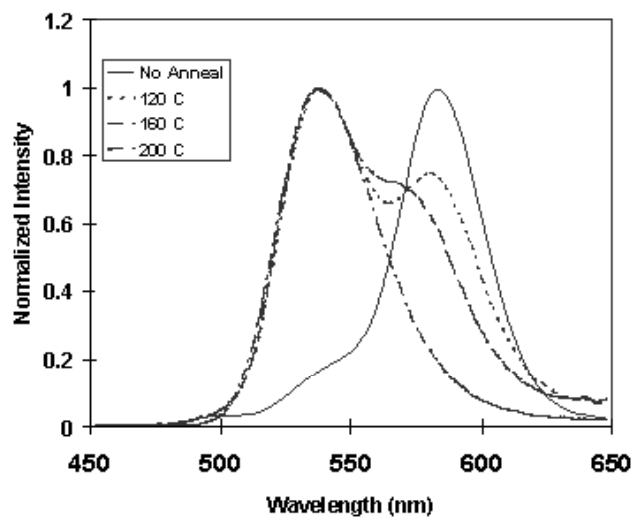

Figure 2. The luminescence spectra from an RIA microcrystal dispersion after annealing at various temperatures for 1 h.

homogeneous iodide luminescence band remains, indicating that the RIA region is lost. The luminescence from RIA microcrystals after a 200 ºC anneal for 1 h is characteristic of microcrystals with a homogeneous level of iodide between 3 and 10%. In contrast, only a slight shift of the luminescence band to shorter wavelengths is seen with increasing annealing temperature in the homogeneous iodide microcrystals.

Figure 3 shows a plot of the band-gap energies of $AgBr_{1-x}I_x$, as a function of iodide concentration (x) at both 4 and 300 K. The gap energy (2.35 ± 0.05 eV @ 4 K) determined from the RIA luminescence by analyzing the excitation spectra were arbitrarily placed at x = 0.9 in Fig. 3. The band-gap energy for "rock salt," δ-AgI, at 4 K is estimated using the difference in band-gap energy at 4 and 300 K for the $AgBr_{1-x}I_x$ samples. The data shown in Fig. 3 indicate the band-gap energies are a monotonically decreasing function of the mole fraction of iodide. These data also indicate that the value of the band-gap energy obtained from the RIA luminescence is suggestive of these regions being (rock salt) δ−AgI.

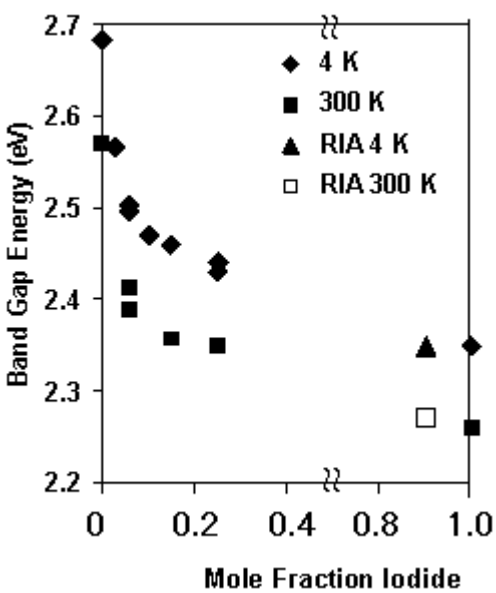

Figure 3. The band-gap energies from various $AgBr_{1-x}I_x$ samples, as a function of the mole fraction iodide, the high-pressure δ-AgI (from literature), and the species found in RIA microcrystals are referenced at 1.0 and 0.9 mole fraction iodide, respectively.

Measured band-gap energies for the known forms of AgI and other fcc silver halides are shown in Table 1.[16,17] A consideration of these energies and the data in Fig. 3 indicate that the best match for the species formed with a "nonequilibrium" addition of iodide (i.e., an RIA procedure) is δAgI or, more realistically, a $AgBr_{1-x}I_x$ region where x is close to 1. The only other possible species might be αAgI, which should only be stable above 417 K. If this species were to exist at low temperature, its band-gap energy could be estimated. Using the known temperature dependence of γAgI and the various $AgBr_{1-x}I_x$ samples, the band-gap energy of αAgI would be placed at about 2.55 eV eV at 4 K, which is inconsistent with the measured band-gap energies near 2.35 eV for the RIA materials.

Table 1. Measured band-gap energies (eV) for various forms of AgI, $AgBr_{.75}I_{.25}$ and AgBr.

T (K)	αAgI (bcc)	βAgI (hcp)	γAgI (zb)	δAgI (fcc)	AgBrI (fcc)	AgBr (fcc)
4		3.023	2.91	2.35 (est.)	2.44	2.71
300			2.82	2.26	2.34	2.57
>420	2.40					

Fabrication of microcrystals with homogeneous iodide regions can induce the formation of stacking fault defects with an *a*/6[1$\underline{2}$1] displacement vector.[18,19] Under a low magnification imaging condition in TEM, these defects are manifested as striation contrast bands running parallel to the microcrystal edges [Fig. 4(a)]. In RIA microcrystals, at least two other structural defects caused by the rapid addition of iodide have been documented. The first is coincident with the crystal growth point at which iodide is rapidly added, resulting in the formation of an edge dislocation positioned concentrically parallel to the microcrystal edges [Fig. 5(a)]. This line exhibits diffraction contrast consistent with a defect core characterized with a Burgers vector value of *a*/6[1$\underline{2}$1].[20] The second defect is a collection of short dislocation segments that start from the rapid iodide addition dislocation line and extends a short distance through the AgBrI perimeter region out to the edge of the microcrystal. ($\underline{2}$02) Two-beam dark-field image analyses indicates that these contain a core structure with mainly *a*/2[$\underline{1}$01] characteristics.[18]

Annealing studies have provided additional insight into the relationships among these structural defects. Annealing homogeneous iodide microcrystals induced a gradual reduction of the stacking faults starting at ~160 °C, followed by their disappearance by 220 °C. By 200 °C, only the stacking fault marking the boundary between the pure AgBr core and the AgBr/I shell remained [Fig. 4(b) and (c)]. By comparison, heating the RIA microcrystals to ~160 °C caused some reduction to the intensity of the *a*/6[1$\underline{2}$1] dislocation lines, but by 200 °C, this feature was completely annealed away. However, no discernible effect on the *a*/2[$\underline{1}$01] dislocation segments was observed [Fig. 5(b) and (c)].

Analytical electron microscopy (AEM) analysis was used to monitor iodide movement associated with annealing. Local iodide content at various locations (A, B, C, and D in Figs. 4 and 5) within individual microcrystals was probed. For homogeneous iodide crystals, the data

indicated a slight increase (0.5 mol %, although this is within experimental

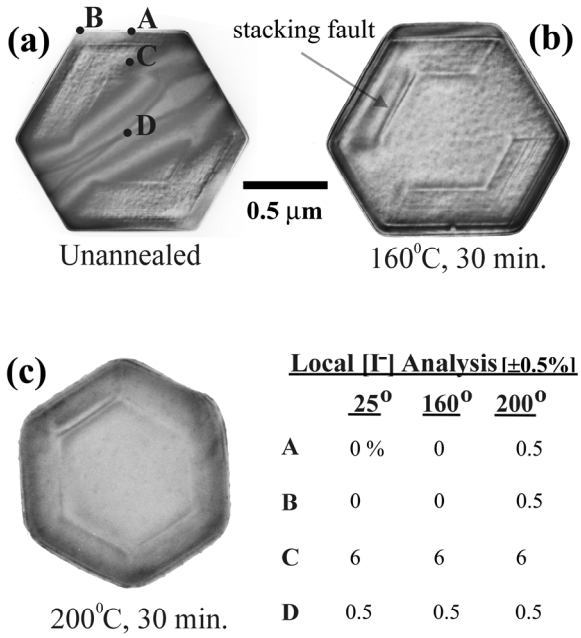

Local [I⁻] Analysis [±0.5%]

	25°	160°	200°
A	0 %	0	0.5
B	0	0	0.5
C	6	6	6
D	0.5	0.5	0.5

Figure 4. Annealing study of microcrystals with homogeneous iodide regions. TEM images showed the striation contrast defects in these tabular crystals anneal away by ~200 ºC. Note the crystals in (a) and (b) were imaged under (2̲02) two-beam conditions. [I] analysis by AEM used a 20 nm probe beam.

error) in iodide content in the pure AgBr region after annealing [Fig. 4(d)]. Similarly, in RIA microcrystals, no significant iodide movement was detected [Fig. 5(d)]. Attempts to monitor the size of, and changes to, the high iodide region at the *a*/6[12̲1] dislocation lines in RIA microcrystals did not consistently show any experimentally significant iodide variation after annealing. Considering the size of the electron beam, and various beam-solid interactions, this technique may not be sensitive enough to determine any short-range iodide movement smaller than ~40 nm.

The *a*/6[12̲1] edge dislocation in RIA AgBrI was further analyzed because of its apparent correlation to the 580 nm LTPL band. TEM results suggest a possible location and also define the probable size of this feature. The similarity in both diffraction contrast and the annealing characteristics of the homogeneous iodide regions, when compared to that of the *a*/6[12̲1] edge dislocation in the RIA microcrystal, is highly suggestive of similar origins. Previous microscopy results have indicated that the stacking faults, observed as striation contrast features in Fig. 4(a), are located on the internal twin planes and are manifested as small regions of multiply-twinned inclined planes.[19] Also, the grid-like dislocation network and its previous linkage to closely spaced jogs on the internal twin planes is suggestive of a location.[11,19] All three defects, the stacking fault

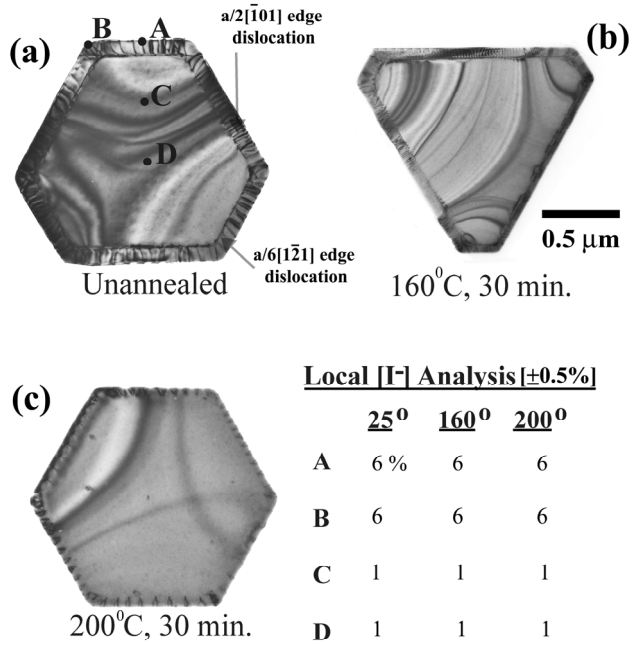

Local [I⁻] Analysis [±0.5%]

	25°	160°	200°
A	6 %	6	6
B	6	6	6
C	1	1	1
D	1	1	1

Figure 5. Annealing study of RIA microcrystals. TEM images show that only the a/6[12̲1] dislocation defects in these crystals anneal away by ~200 ºC. The a/2[1̲01] dislocation segments were not affected by annealing. [I] analysis used a 20 nm probe beam.

and dislocation network of the homogeneous material and the edge dislocation in RIA, exhibit the same zero contrast property when imaged under the (2̲02) two-beam condition in the TEM. This suggests that the latter is also a structural defect on the internal twin planes of RIA tabular microcrystals. This is further substantiated by the annealing results. The removal of the *a*/6[12̲1] dislocations at ~200 °C in the RIA microcrystals, compares similarly to the loss of the multiple striation contrast (from the stacking faults) and the grid-like contrast features in homogeneous iodide microcrystals when annealed,[11] and points to the similar core structure between these three defects in the AgBr/I lattice.

Additional evidence on the location of these defects on the twin planes is the reported finding that, accompanying the loss of striation-like fringes in homogeneous iodide microcrystals, is the transformation of the twin planes from a jagged to a smooth morphology after a 200 ºC annealing treatment.[11] Hence, the *a*/6[12̲1] dislocation feature in RIA microcrystals is likely located on the internal twin planes as a step or jog.

Direct evidence of the *a*/6[12̲1] dislocation as a perturbation to the twin planes has been found in cross-sections of RIA microcrystals. Under low magnification conditions, with electron beam carefully aligned along [10̲1], two distinct features have been found. First, a

concentric, linear feature inside the tabular microcrystal is seen, labeled as "RIA boundary" [Fig. 6(a)]. AEM analysis on this line indicates a relatively high iodide concentration ranging from 12–18 mol %. While this data shows the RIA boundary line corresponding to a region of high [I], it does not have the spatial resolution to discriminate the actual [I] at the center or core of this line. However, it is likely that the core of the RIA boundary has a much higher [I] than 12–18 mol % iodide measured. Given its proximity to a pure AgBr region, it is possible that the small core is nearly pure AgI. High magnification and electron diffraction studies did not reveal another structural phase in the RIA boundary region. The morphology of this region suggests that TEM is imaging a strained field around the core, which is isostructural with the fcc AgBr matrix, yet its lattice constant is significantly different. One possible core structure would be the high-pressure phase form of AgI, which has a rock salt lattice, with a lattice parameter that is ~10% larger than that of AgBr.

The second intriguing feature noted is at the intersection of the high-iodide RIA boundary with the twin planes. It is noted that at this intersection, a job/step on the twin boundary occurs on at least one of the twin planes [Fig. 6(b)]. Previously, it had been proposed that an *a*/6[1$\underline{2}$1]

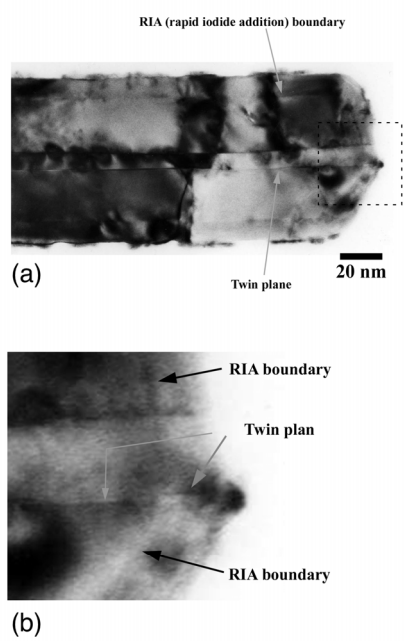

Figure 6. (a) A TEM image of a cross-sectioned segment of a tabular RIA microcrystal, collected with the beam aligned in order to observe the (111) twin-plane edge. A lattice distortion region coincident with the rapid incorporation of iodide is seen. (b) Enlargement of the inset from (a) showing details of the intersection of the RIA boundary with the twin plane.

twinning dislocation on the twin boundary is a spatial offset across the twin plane by n/2 of the (111) spacing, where n is an odd integer.[21] In combination, this additional evidence suggests that the core of such a jog is a nanoregion of pure AgI. This region is expected to be very small, ~ two (111) layers thick, one on either side of the jog, or ~0.63 nm. Such a small region of AgI is consistent with the lack of diffraction or stoichiometric quantification, as discussed earlier. The offset, caused by the *a*/6[1$\underline{2}$1]-twinning dislocation seen in these cross-sections, corresponds to the linear feature identified as the *a*/6[1$\underline{2}$1]-edge dislocation in plan-view images, Fig. 5(a). However, the related *a*/2**[$\underline{1}$01]** short dislocation segments seen in plan-views would extend from the jog on the twin boundary toward the outer edge of the crystal. Because these lie on the twin boundary, they are obscured by the contrast of this planar feature, and therefore, are not directly visible in cross-section images. The geometry of these two dislocations is consistent with that first proposed by Hamilton.[21]

The experimentally observed removal of this dislocation or jog on the twin boundary at 200 °C [Fig. 5(c)], coincident with the loss of the 580 nm LTPL luminescence, indicates a short-range movement of the atoms at the twinning dislocation. It is most likely that the change to the twin plane is the removal of the jog to form a straight twin-plane boundary line, similar to that demonstrated for homogeneous iodide, AgBrI.[11] This evidence of atomic rearrangements also points to the possibility that the small, high-iodide regions can relax and diffuse into the surrounding lattice in the RIA boundary line, thus removing the "cause" of the 580 nm luminescence.

The question of the existence of a high-pressure phase can be discussed from several points of view. Certain epitaxial thin layers have been known to adopt the crystal structure of the host substrate even under considerable elastic strain.[22] Thus, it might be expected that very small regions of silver iodide might take the crystal structure of the host, i.e., fcc (rock salt) instead of the ambient temperature and pressure phases which are hcp (wurtzite) and fcc (zincblende). Further, the lattice mismatch will cause an effective pressure on that region making a "high pressure" phase more likely. The pressure can be estimated from classical considerations resulting from the negative derivative with respect to the volume of an attractive Madelung potential containing an exponential repulsive term.[23] Substituting known constants[7] and assuming that the AgBr lattice does not distort, the calculated pressure is of the same order of magnitude as the phase transition pressure required to convert AgI to the rock salt phase δ-AgI. While this is a classical picture, the Madelung potential predicts lattice energies to better than 10% and should produce a reasonable estimate of the pressure (strain) in the lattice. The formation of strained regions after a rapid addition iodide step with continued precipitation of the parent material suggests a general mechanism for the formation of certain dislocations associated with RIA microcrystals.

Another way to look at the internal "pressure" is to consider the strain near an AgI cluster. The computational

question is whether a small region of δ−AgI could be stable within the AgBr crystal. AgI ion pairs were substituted for AgBr in spherical arrays containing AgI_6, AgI_6Ag_{12}, and $AgI_6Ag_{12}I_8$. After relaxation, the AgI cluster remained in the rock salt structure in all of these cases. The Ag-I bond length was elongated by up to 0.1 Å over the normal Ag-Br bond length of 2.864 Å. Cubic and rectangular clusters of ions including Ag_6I_6 (3 × 2 × 2), Ag_9I_9 (3 × 2 × 3), $Ag_{13}I_{14}$ (3 × 3 × 3), $Ag_{18}I_{18}$ (4 × 3 × 3), and $Ag_{37}I_{38}$ (5 × 5 × 3) were considered next. Again, the relaxed structure remained rock salt with displacements from the original AgBr sites of up to about 0.15 Å. In the case of the largest cluster, the Ag-I bond lengths were up to 0.15 Å greater than AgBr, but the displacement off cubic sites was less than 0.01 Å. In no case did we observe a change to wurtzite structure, even though the AgI potential is for a wurtzite crystal structure.

Subsequently, tetrahedral AgI_4 (wurtzite units) were substituted for $AgBr_6$. This structure relaxed back to nearly the octahedral sites of the rock salt structure. Of course, a perfect octahedral structure would not be expected because of the presence of two vacancies. A larger $Ag_{13}I_{14}$ cluster in the wurtzite structure substituted for various sized AgBr clusters in order to provide sufficient space for the AgI cluster was also studied. In all cases, the computations were unable to find a stable wurtzite structure of AgI within the fcc AgBr. These computations indicate that small regions of fcc rock salt δ−AgI are stable in an AgBr lattice.

Conclusions

This investigation has detailed the experimental and theoretical observations pertaining to the structure created when iodide, either as a KI solution or as AgI nanocrystals, is added rapidly during the aqueous precipitation of AgBr microcrystals with a gelatin peptizer. LTPL has identified a luminescence "species" specific to AgBr(I) microcrystals that results from a RIA procedure. Extrapolations of measured band-gap energies strongly suggest that the luminescence species are related to small regions of an almost pure δAgI phase specifically rock salt AgI. Simple assumptions using Madelung potential energy calculations suggest that small regions of δAgI confined within an AgBr lattice result in localized pressures comparable to the formation pressures required for formation of bulk δ-AgI. Computations indicate that small regions of δ-AgI are stable in an fcc AgBr lattice structure. Computations further indicate that small regions of hcp (wurtzite) AgI in a rock salt AgBr lattice are "unstable."

Detailed microstructure analysis by TEM suggests the likely presence of a high iodide region inside the AgBrI crystal coinciding with the introduction of AgI (or KI) during the crystal preparation process. Structural analysis of the dislocations induced by the rapid addition of iodide points to the presence of a high iodide rock salt structure at its core. It is likely centered in the RIA region and is the source of the 580 nm LTPL in AgBr/I microcrystals. In tabular microcrystals, the intersection between the RIA boundary and the internal twin planes generates a jog/step on the twin plane that has been observed. Such structural elements are suggestive of the size of such a core region, and may only be ~0.6 nm thick. Annealing to 200 °C removes the *a*/6[1$\underline{2}$1] dislocation coincident with the disappearance of the 580 nm LTLP band. This suggests short-range atomic movement can occur to "dilute" the AgI core to blend into its isostructural AgBrI matrix.

References

1. J. Solberg *et al.,* U.S. Patent 4,433.048 (1984); H. Wilgus *et al.*, U.S. Patent 4,434.226 (1984);
2. O. Stasiw and J. Teltow, *Z. Anorg. Chem.*, **249**, 143 (1949).
3. A. P. Marchetti and M. S. Burberry, *Phys. Rev. B*, **37**, 10862 (1988).
4. A. P. Marchetti and M. S. Burberry, *Phys. Rev. B*, **28**, 3130 (1983).
5. M. G. Mason, Y. T. Tan, T. J. Miller, G. N. Kwawer, F. C. Brown, and A. B. Kunz, *Phys. Rev. B*, **42**, 2996 (1990).
6. E. Chang et al., U.S. Patent 5,314,793 (1994) and U.S. Patent 5,360,703 (1994); X. Wen, U.S. Patent 5,470,698 (1995); S. H. Ehrlich, *J. Imaging Sci. Technol.*, **37**, 73 (1993).
7. A. P. Marchetti, J. C. Hansen, S. Chen, M. Irving, R. Baetzold, and B. R. Sever, *Phys. Rev. B*, **69**, 94107 (2004).
8. M. Irving et al., U.S. Patent 5,728,515 (1998).
9. A. P. Marchetti, P. J. Rodney, and W. von der Osten, *Phys. Rev. B*, **64**, 132201 (2001).
10. S. Ves, D. Glotzel, M. Cardona, and H. Overhof, *Phys. Rev. B*, **24**, 3073 (1981).
11. S. Chen, A. E. Taddei, J. Jagannathan, and M. G. Antoniades**,** *J. Imaging Sci. Technol.*, **45**, 230 (2001).
12. R. C. Baetzold, *J. Phys. Chem. Solids*, **57**, 627 (1996).
13. R. C. Baetzold, *Phys. Rev. B*, **52**, 11424 (1995).
14. C. R. A. Catlow, J. Corish, J. H. Harding, and P. W. M. Jacobs, *Philos. Mag.*, A **55**, 481 (1987).
15. J. D. Gale, *J. Chem. Soc. Faraday Trans.*, **93**, 69 (1997).
16. O. Madelung Ed, *Semiconductors other than Group IV and III-V compounds*, Springer-Verlag, Berlin, 1992.
17. W. von der Osten, I–VII Compounds in *Landolt–Börnstein, New Series Vol. 17b*., Springer–Verlag, Berlin, 1982, pp. 273–296.
18. C. Goessens, D. Schryvers, J. Van Landuyt, S. Amelinckx, A. Verbeeck, and R. De Keyzer, *J. Cryst. Growth*, **110**, 930 (1991).
19. S. Jagannathan, S. Chen, R. V. Mehta, and R. Jagannathan, *Phys. Rev. B*, **53**, 9 (1996).
20. W. Van Renterghem, S. Karthauser, D. Schryvers, J. Van Landuyt, R. De Keyzer, and C. Van Roost, *Proc. Int. Symp. Silver Halide Imaging*, pg. 167.
21. J. F. Hamilton, *Philos. Mag*., **16**, 1 (1967).
22. A. P. Sutton and R. W. Balluffi*, Interfaces in Crystalline Materials*, Oxford University Press, New York, 1996, pg. 108.
23. M. Born and K. Huang, *Dynamical Theory of Crystal Lattices*, Oxford, University Press, London, 1966, pg. 24ff.